Title
Phase Behavior of a Block Copolymer/Salt Mixture through the Order-to-Disorder Transition

Journal
Macromolecules, 47(8)

ISSN
0024-9297

Authors
Thelen, Jacob L
Teran, Alexander A
Wang, Xin
et al.

Publication Date
2014-04-22

DOI
10.1021/ma500292n

Peer reviewed

Macromolecules

Article

pubs.acs.org/Macromolecules

Phase Behavior of a Block Copolymer/Salt Mixture through the Order-to-Disorder Transition

Jacob L. Thelen,[†,‡] Alexander A. Teran,[†,‡] Xin Wang,[§] Bruce A. Garetz,[§] Issei Nakamura,[⊥,#] Zhen-Gang Wang,[⊥] and Nitash P. Balsara[†,‡,∥,*]

[†]Department of Chemical and Biomolecular Engineering, University of California, Berkeley, California 94720, United States

[‡]Environmental Energy Technologies Division, Lawrence Berkeley National Laboratory, Berkeley, California 94720, United States

[§]Department of Chemical and Biomolecular Engineering, NYU Polytechnic School of Engineering, Brooklyn, New York 11201, United States

[⊥]Division of Chemistry and Chemical Engineering, California Institute of Technology, Pasadena, California 91125, United States

[∥]Materials Sciences Division, Lawrence Berkeley National Laboratory, Berkeley, California 94720, United States

Supporting Information

ABSTRACT: Mixtures of block copolymers and lithium salts are promising candidates for lithium battery electrolytes. Structural changes that occur during the order-to-disorder transition (ODT) in a diblock copolymer/salt mixture were characterized by small-angle X-ray scattering (SAXS). In salt-free block copolymers, the ODT is sharp, and the domain size of the ordered phase decreases with increasing temperature. In contrast, the ODT of the diblock copolymer/salt mixture examined here occurs gradually over an 11 °C temperature window, and the domain size of the ordered phase is a nonmonotonic function of temperature. We present an approach to estimate the fraction of the ordered phase in the 11 °C window where ordered and disordered phases coexist. The domain spacing of the ordered phase increases with increasing temperature in the coexistence window. Both findings are consistent with the selective partitioning of salt into the ordered domains, as predicted by Nakamura et al. (*ACS Macro Lett.* **2013**, *2*, 478−481).

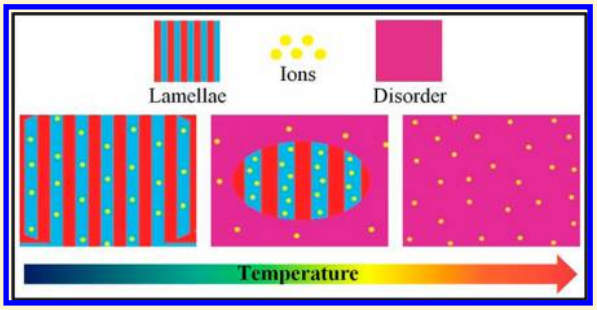

INTRODUCTION

Lithium metal batteries utilizing solid polymer electrolytes (SPEs) have recently gained considerable interest for use in electrified transportation applications.[1] In particular, block copolymer-based SPEs have demonstrated the remarkable ability to efficiently conduct lithium ions while preventing lithium dendritic growth,[2] a problem that has plagued the implementation of lithium metal batteries since their initial commercial development in the 1980s.[3] Block copolymer electrolytes gain their unique properties by self-assembling into ordered arrays of hard, mechanically robust and soft, ion-conducting nanoscale domains.[4] At sufficiently high temperatures, entropy overcomes the repulsive forces between the chemically distinct polymer blocks and a homogeneous disordered phase is obtained. The transition from order to disorder is thus of considerable practical and fundamental significance.

The order-to-disorder transition (ODT) in neat A−B diblock copolymer melts is well understood. We restrict our attention to nearly monodisperse samples, which are, to a good approximation, one component systems. The mean field theory of Leibler predicts that for symmetric block copolymers wherein the volume fraction of the A-block (f_A) is 0.5, the ODT occurs at the temperature at which $\chi N = 10.495$, where χ is the temperature-dependent Flory−Huggins interaction parameter between segments A and B, and N is the number of segments per chain.[5] Small angle X-ray scattering (SAXS) has emerged as a powerful tool for studying the ODT in block copolymers. The disordered phase is characterized by a broad SAXS peak due to correlations between A and B segments enforced by connectivity, while the ordered phase is characterized by sharp peaks consistent with the symmetry of that phase. The SAXS signatures of the ODT have been reported in numerous publications.[6−12] Both the width and the height of the primary SAXS peak change discontinuously at the ODT. In contrast, the position of the primary peak (q^*) and the integrated scattering intensity (Q) decrease monotonically with increasing temperature with virtually no evidence of discontinuity at the ODT.

The mean field theory of Leibler predicts that the ODT of symmetric block copolymers is second-order.[5] Subsequent work by Fredrickson and Helfand[13] showed that fluctuations in the disordered state result in a change to a weakly first-order

Received: February 6, 2014
Revised: March 17, 2014
Published: April 2, 2014

   dx.doi.org/10.1021/ma500292n | *Macromolecules* 2014, 47, 2666−2673

Table 1. Sample Characteristics

sample name	M_{PS} (g mol^{-1})	M_{PEO} (g mol^{-1})	PDI	$f_{EO,eff}$[a] (140 °C)	T_g^{PS} (°C)	r ([Li$^+$][EO]$^{-1}$)
SEO(1.7−1.4)/LiTFSI (r = 0.075)	1700	1400	1.05	0.50	30	0.075
SEO(6.4−7.3)	6400	7300	1.04	0.52	80	0

[a]Effective volume fraction of PEO/LiTFSI component based on calculation described in ref19.

phase transition, consistent with a note in Leibler's original paper. The mean field limit is recovered in the limit of $N \rightarrow \infty$.

The effect of added salt on block copolymer thermodynamics is a relatively new and unexplored topic. Early experiments suggested that the thermodynamics of block copolymer/salt mixtures can be described by the same theories that were used to describe neat block copolymers except for the fact that χ must be replaced by an effective parameter (χ_{eff}) that now depends on salt concentration.[14−17] Generally speaking, with notable exceptions,[18,19] χ_{eff} was found to be larger than χ of the neat block copolymer, suggesting that the addition of salt stabilizes the ordered phase. The thermodynamic consequences of this were worked out by Nakamura et al.[15,16,20] They argued that as the ODT progressed, salt would partition preferentially into the ordered phase, leaving behind a disordered phase with lower salt concentration.[20] At equilibrium, the chemical potential of the salt in the two phases will be equal, dictating the compositions and morphologies of the coexisting disordered and ordered phases. This changes the order of the ODT and a first-order transition is obtained even in the mean field limit for any N, consistent with the Gibbs phase rule for binary mixtures.

The purpose of this paper is to report on the phase behavior of a block copolymer/salt mixture through the ODT using SAXS. We show that the SAXS signatures of the ODT of these systems are qualitatively different from those of neat diblock copolymers. The work presented here builds upon the results obtained by Wanakule et al.[14]

EXPERIMENTAL SECTION

Materials. The polystyrene-*b*-poly(ethylene oxide) (SEO) diblock copolymers used in this study were synthesized, purified, and characterized following the methods described in refs 21, 22, and 23. The polymer characteristics are summarized in Table 1. The polymers were dried under vacuum at 90 °C for 24 h before being stored in an argon-filled glovebox (MBraun) with sub ppm water and oxygen levels. Lithium bis(trifluoromethanesulfonyl)imide (LiTFSI) was obtained from Novolyte. The LiTFSI container was opened inside the glovebox, and then dried in a heated antechamber under vacuum for 3 days at 120 °C before being stored in the argon glovebox.

Sample Preparation. The polymer/salt mixture used in this study was prepared by mixing SEO(1.7−1.4)/benzene and LiTFSI/tetrahydrofuran (THF) solutions to obtain a salt concentration of r = 0.075 where r is the ratio of Li$^+$ ions to ethylene oxide monomer units. The SEO(1.7−1.4)/LiTFSI(r = 0.075) solution was freeze-dried in a Millrock LD85 lyophilizer to remove the solvent. The SEO(1.7−1.4)/LiTFSI(r = 0.075) mixture was returned to the glovebox antechamber without being exposed to air and dried under vacuum at 90 °C for 24 h to remove any residual solvent.

Three *in situ* SAXS samples were prepared by melt forming the dried SEO(1.7−1.4)/LiTFSI(r = 0.075) mixture into a $^1/_{16}$ in. thick fiberglass reinforced silicone spacer with a diameter of $^3/_{16}$ in. Both ends of the spacer were sealed with electrochemical grade aluminum foil electrodes, and then each sample was sealed in a vacuum pouch (Showa-Denka) with exposed aluminum tabs contacting each electrode. An empty pouch cell was also prepared in the same manner to serve as a blank reference for SAXS background subtraction. All of the samples were heated to 140 °C to eliminate any strain induced during sample preparation and then cooled to and annealed at 70 °C for 20 h and then at 50 °C for 20 h before being stored at 30 °C. The *in situ* SAXS measurements were performed after two days of storage at 30 °C.

SAXS Measurements. SAXS measurements were performed at Lawrence Berkeley National Laboratory's Advance Light Source, beamline 7.3.3.[24] The sample-to-detector distance and beam center were calibrated using a silver behenate standard. The three SEO(1.7−1.4)/LiTFSI(r = 0.075) samples and the empty cell were mounted onto a custom-built heating stage with thermocouples attached to both the front and back of each sample. An Omega OM-USB-TC data acquisition module was used to record each sample temperature every 10 s. The samples were connected to a Bio-Logic VMP3 potentiostat through the aluminum tabs contacting each electrode. Electrochemical impedance spectroscopy (EIS) measurements were performed over a 1−10^6 Hz frequency range with 50 mV amplitude.

The samples were equilibrated at 29 °C for 1 h in the SAXS instrument before beginning the heating scan. The heating scan was performed from 29 to 142 °C. Five °C temperature steps were used for temperatures far from the ODT (29−78 °C and 107−142 °C), and the samples were held at each temperature for a minimum of 30 min while EIS and SAXS measurements were performed every 10 min. Smaller temperature steps were used near the ODT (78−91 °C). In this case, 2−3 °C steps were used and again the samples were held for a minimum of 30 min with EIS and SAXS scans performed every 10 min. 1 °C temperature steps were used for the window of 93−104 °C and the samples were held at each temperature for at least 1 h with EIS and SAXS scans performed approximately every 10 min.

Each sample temperature was determined from the average of their front and back thermocouple readings during the scan; the back thermocouple was located adjacent to the heating element and it records the maximum possible sample temperature, while the front thermocouple reading represents the minimum possible temperature. Sample temperatures are reported with error bars corresponding to these readings. The actual sample temperature was estimated by making separate electrolyte samples with a thermocouple running through the pouch. In all cases, the recorded sample temperature fell within the errors bars described above. The bulk electrolyte resistance was determined from the low frequency minimum of a Nyquist plot of the EIS data. We found that the temperature- and microstructure-dependence of the ionic conductivity for SEO(1.7−1.4)/LiTFSI (r = 0.075) qualitatively agreed with the published data of Teran et al.[25] The data are provided in Figure S1 of the Supporting Information. This paper is based exclusively on the SAXS data.

SAXS Data Reduction and Analysis. The raw SAXS patterns were reduced using the Nika macro for Igor Pro developed by Jan Ilavsky.[26] The scattering intensity (I) was averaged azimuthally and is reported as a function of the magnitude of the scattering vector, $q = (4\pi/\lambda)\ \sin\ (\theta/2)$. Reduced SAXS data were further processed by subtracting the background scattering from the empty sample cell, and calibrated to a glassy carbon absolute intensity standard (sample M13, Jan Ilavsky). Standard deviation of the scattering intensity was approximated by the Nika reduction software and then propagated through the subsequent reduction steps with the assumption of uncorrelated random error.

Contributions to the absolute scattering intensity at each temperature were determined by nonlinear fitting of the scattering profiles. We utilized the built-in Levenberg−Marquardt nonlinear least-squares algorithm in Igor Pro with a user defined function to deconvolute the scattering into three components using eq 1:

$$I_{tot}(q) = I_{ord}(q) + I_{dis}(q) + I_{bgd}(q) \quad (1)$$

dx.doi.org/10.1021/ma500292n | Macromolecules 2014, 47, 2666−2673

where I_{tot} is the total measured scattering intensity, and I_{ord}, I_{dis}, and I_{bgd} are the scattering intensities due to the nanostructured ordered phase, the disordered phase, and the background, respectively. A Gaussian fuction was used to fit the primary ordered scattering peak:

$$I_{ord}(q) = y_0 e^{(-(q-q^*)^2/2w^2)} \quad (2)$$

Here y_0, w, and q^* are the primary scattering peak height, width, and position, respectively. The well-known Leibler structure factor[5] modified for polydispersity effects[9] was used to fit the broad disordered scattering peak:

$$I_{dis}(q) = C\left[\frac{S(q)}{W(q)} - 2\chi_{eff}\right]^{-1} \quad (3)$$

with

$$C = {}_{ref}\left(\frac{b_A}{\nu_A} - \frac{b_B}{\nu_B}\right)^2_{eff} \quad (4)$$

$$S(q) = S_{AA}(q) + S_{BB}(q) + 2S_{AB}(q) \quad (5)$$

$$W(q) = S_{AA}(q)S_{BB}(q) - S_{AB}{}^2(q) \quad (6)$$

$$S_{AA}(q) = Ng(f_A) \quad (7)$$

$$S_{BB}(q) = Ng(1 - f_A) \quad (8)$$

$$S_{AB}(q) = \frac{N}{2}[g(1) - g(f_A) - g(1 - f_A)] \quad (9)$$

and

$$g(f) = 2(1/x^2)\{fx - 1 + [k/(k + fx)]^k\} \quad (10)$$

where

$$x = q^2 R_g{}^2 \quad (11)$$

and

$$k = \frac{1}{\mathrm{PDI} - 1} \quad (12)$$

C is the effective scattering contrast from the difference in electron density between component A and component B, χ_{eff} is the effective interaction parameter, f_A is the volume fraction of block A, R_g is the radius of gyration, N is the number of polymer segments per chain, and PDI is the polydispersity index of the copolymer. The background scattering was fit with a decaying exponential function:

$$I_{bgd}(q) = y_1 e^{(y_2/q)} \quad (13)$$

where y_1 and y_2 are constants. Fitting was performed with y_0, q^*, w, C, R_g, χ_{eff}, y_1, and y_2 as the adjustable parameters. Figure 1 shows a typical scattering profile and fit for a SEO(1.7−1.4)/LiTFSI(r = 0.075) sample when both ordered and disordered phases coexist. The contributions from I_{ord}, I_{dis}, and I_{bgd} are also shown in Figure 1, offset by a decade for clarity. The fit parameters obtained for this scattering profile are given in Table S1 of the Supporting Information, and those for all other temperatures are also provided in Tables S2−4 of the Supporting Information.

The fit parameters were used to calculate the characteristic domain spacing of the ordered phase, d_{ord},

$$d_{ord} = \frac{2\pi}{q^*} \quad (14)$$

and the characteristic length-scale of the disordered fluctuations, d_{dis},

$$d_{dis} = \frac{2\pi R_g}{\sqrt{3.6}} \quad (15)$$

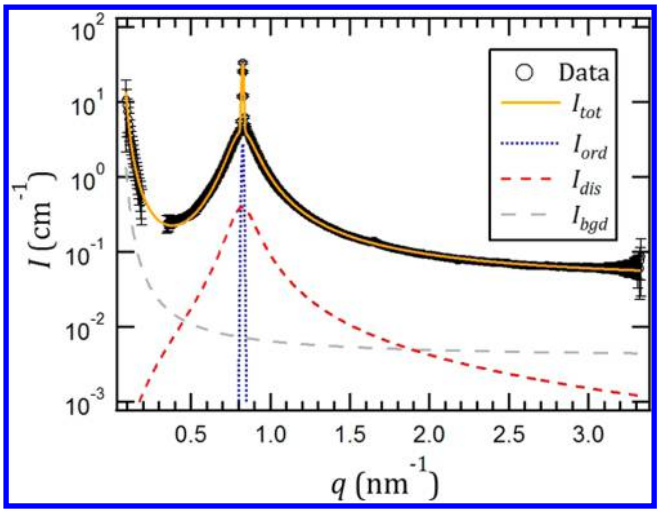

Figure 1. Example data and fitting for an SEO(1.7−1.4)/LiTFSI(r = 0.075) sample during phase coexistence (97 °C). Experimental data are shown as discrete points with black circles and error bars corresponding to one standard deviation. The total fitting curve (I_{tot}) is plotted as a solid yellow line. The three contributions to the fit are shown as dashed lines offset by a decade with I_{ord} in blue, I_{dis} in red, and I_{bgd} in gray. Note: Data between q = 0.198 and q = 0.348 nm^{-1} correspond to a peak in the background (empty sample) scattering. Imperfect background subtraction resulted in negative and near zero intensity values within this range, and thus the data are not shown.

where R_g is obtained by the fitting procedure (equ 1-13), and the factor $(3.6)^{1/2}$ was determined using the methodology described by Teran et al.[19] The fitted curves were used to calculate the scattering invariant (Q_i), defined as

$$Q_i = \int I_i(q)q^2\,dq \quad (i = ord \text{ or } dis) \quad (16)$$

For a heterogeneous system with two distinct phases separated by sharp interfaces, the invariant is independent of morphology and depends only on the volume of one of the phases.[27] In this case, $I \propto q^{-4}$ as $q \to \infty$ and the invariant is well-defined. It is well-known that $I_{dis} \propto q^{-2}$ as $q \to \infty$, and thus Q_{dis} is unbounded. We define ΔI_{dis} as

$$\Delta I_{dis} = I_{dis} - I_{dis,\chi=0} \quad (17)$$

where $I_{dis}\chi_{=0}$ is calculated by using the fit parameters determined for I_{dis}, but setting χ_{eff} = 0 in eq 3. In Figure 2 we plot $\Delta I_{dis}q^2$ vs q for the data shown in Figure 1. The inset in Figure 2 shows the q-dependence of $I_{dis}q^2$ and $I_{dis}\chi_{=0}q^2$. It is clear from Figure 2 that ΔQ, defined as

$$\Delta Q = \int \Delta I_{dis}(q)q^2\,dq \quad (18)$$

is bounded.

Because Q_{ord} and ΔQ depend only on the volumes of the ordered and disordered phases, respectively, we assume they are proportional to the volume of each phase, so that the volume fraction of the ordered phase (ϕ_{ord}) is given by

$$\phi_{ord} = \frac{Q_{ord}}{Q_{ord} + \Delta Q} \quad (19)$$

The values of Q_{ord} and ΔQ determined in this study were obtained from evaluating the integrals in eqs 16 and 18 between the limits q = 0.09 and 3.3 nm^{-1}. Table S5 of the Supporting Information provides the physically relevant values calculated from eqs 14-19 for one of the SEO(1.7−1.4)/LiTFSI(r = 0.075) samples at all measured temperatures.

The data reduction and fitting analysis were performed on the SEO(1.7−1.4)/LiTFSI(r = 0.075) data gathered in the present study, as well as the scattering data collected from neat SEO(6.4−7.3) in the

dx.doi.org/10.1021/ma500292n | Macromolecules 2014, 47, 2666−2673

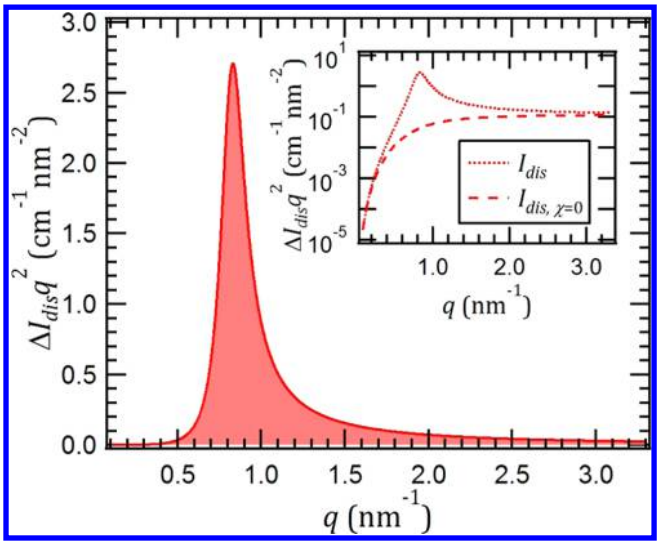

Figure 2. Graphical portrayal of the numerical integration used to calculate the scattering invariant contribution from the disordered phase. Inset: Curves of $I_{dis}q^2$ and $I_{dis}\chi_{=0}q^2$ which were subtracted to yield $\Delta I_{dis}q^2$.

recently published work by Teran et al.[19] Whereas neat SEO (1.7−1.4) has a disordered morphology over all accessible temperatures, neat SEO(6.4−7.3) has a thermally accessible lamellar-to-disorder transition.[19] We compare the ODTs of SEO(1.7−1.4)/LiTFSI(r = 0.075) and neat SEO(6.4−7.3) because they both occur in a similar temperature window (90−105 °C). This temperature window is well above the glass transition temperature of the poly(styrene) block (T_g^{PS}) of each sample; thus, the SAXS measurements made during each ODT should reflect thermodynamic structures.

RESULTS AND DISCUSSION

Temperature-dependent SAXS profiles obtained from one of the SEO(1.7−1.4)/LiTFSI(r = 0.075) sample are shown in Figure 3. At temperatures between 29 and 91 °C, the scattering profiles indicate the presence of a well-ordered lamellar morphology with sharp peaks at positions corresponding to q^*, $2q^*$, and $3q^*$ (blue curves in Figure 3). Data obtained in the

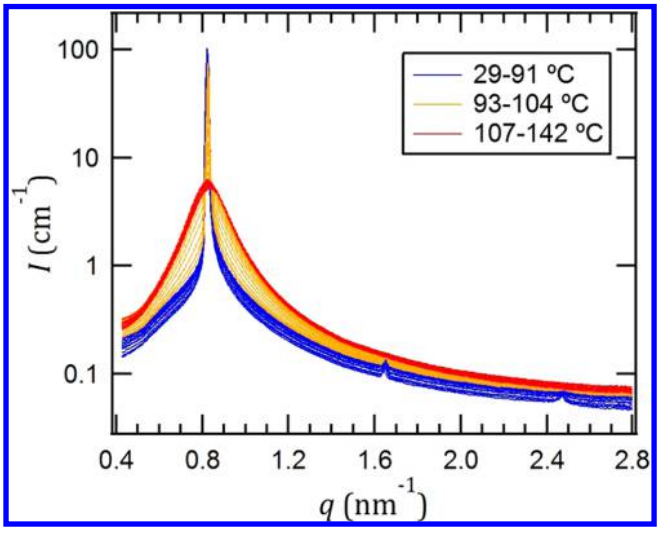

Figure 3. Absolute scattering intensities for SEO(1.7−1.4)/LiTFSI(r = 0.075) from 29 to 142 °C. Blue traces denote well-ordered lamellar structures, yellow traces show coexistence of ordered lamellae and disordered phases, and red traces are fully disordered.

93−104 °C temperature range (yellow curves in Figure 3) are shown on an expanded scale in Figure 4a. Within this temperature range, even small increases (1 °C) in temperature result in large changes in the scattering profile. The general character of the SAXS profiles in this temperature range is clearly seen in the 102 °C data in Figure 4a. This SAXS profile is clearly a superposition of broad and narrow scattering peaks at q = 0.82 nm^{-1}. We attribute this superposition to the coexistence of ordered and disordered phases within the polymer/salt sample. For temperatures above 107 °C, the SAXS profiles contain a single broad peak (red curves in Figure 3), characteristic of fully disordered samples. It is clear that ordered and disordered phases coexist in the polymer/salt sample at temperatures between 93 and 104 °C. In other words, the ODT occurs over a range of temperatures.

The data obtained from SEO(6.4−7.3) were very similar to data obtained from other neat block copolymers in the literature.[6,8,10,11] Temperature-dependent SAXS profiles obtained from the neat SEO(6.4−7.3) sample in the vicinity of the ODT are shown in Figure 4b. It is clear that an increase in temperature from 100 to 105 °C results in an abrupt transition from order to disorder.

The SAXS results described above were used to determine the temperature dependence of ϕ_{ord}, d_{dis}, and d_{ord}. Figure 5a shows the temperature dependence of ϕ_{ord} of the salt-containing block copolymer. The fraction of ordered lamellar phase (ϕ_{ord}) decreases gradually from 0.74 to 0.61 as temperature increases from 29 to 91 °C. At temperatures between 93 and 104 °C, ϕ_{ord} decreases rapidly from 0.59 to 0. Not surprisingly, ϕ_{ord} is identically 0 at temperatures above 107 °C in Figure 5a. The temperature dependence of ϕ_{ord} obtained from the neat block copolymer, shown in Figure 5b, exhibits a discontinuous jump from 0.61 to 0 as the temperature is increased from 100 to 105 °C. This is qualitatively different from the behavior of the salt-containing block copolymer. We note the value of ϕ_{ord} at temperatures well below the ODT is near 0.7 for both samples. One might expect a fully ordered lamellar sample at temperatures well below the ODT to yield ϕ_{ord} = 1. It is well-known that block copolymer lamellae are not pure; i.e., there is a finite concentration of PS chains in the PEO-rich lamellae and vice versa. We expect that scattering from such mixed microphases will be described by theory similar to the random phase approximation.[5,28] This effect results in scattered intensity from the ordered phase that is not accounted for in our analysis. Our results suggest that the contribution from this effect to the overall disordered scattering is about 30%. In other words, we propose that our samples are fully ordered at temperatures well below the ODT temperature in spite of the fact that ϕ_{ord} is less than unity.

Additional information about phase behavior of the polymer melts can be gained by tracking the temperature dependence of the characteristic domain spacing. Figure 5c shows the data obtained from one of the SEO(1.7−1.4)/LiTFSI (r = 0.075) polymer/salt mixtures, where filled symbols correspond to the lamellar spacing calculated from eq 14 (d_{ord}), and open symbols are the characteristic length of the disordered phase calculated from eq 15 (d_{dis}). The temperature dependence of the domain spacing for the polymer/salt mixture displays three distinct regimes, corresponding to the temperature windows for fully ordered, phase coexistence, and fully disordered states. Within the fully ordered temperature range, d_{ord} decreases gradually with increasing temperature (T) between 29 and 81 °C; the slope, $d(d_{ord})/dT$, is -8.35×10^{-4} nm K^{-1}. d_{ord} is independent

dx.doi.org/10.1021/ma500292n | Macromolecules 2014, 47, 2666−2673

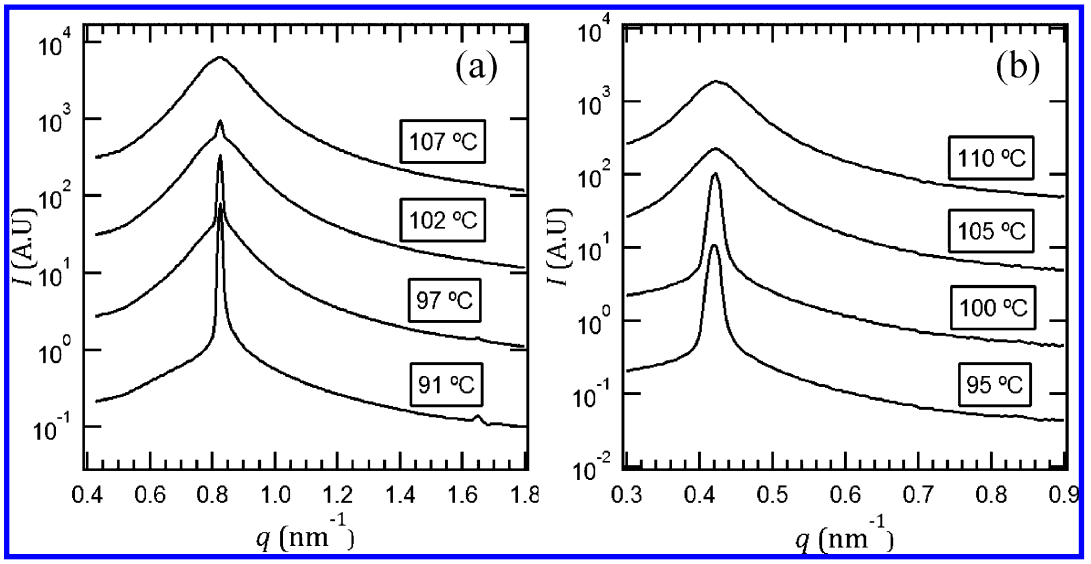

Figure 4. SAXS profiles for (a) SEO(1.7−1.4)/LiTFSI(r = 0.075) through its ODT coexistence window, and (b) SEO(6.4−7.3) below and above its ODT. Profiles are offset by a decade for clarity.

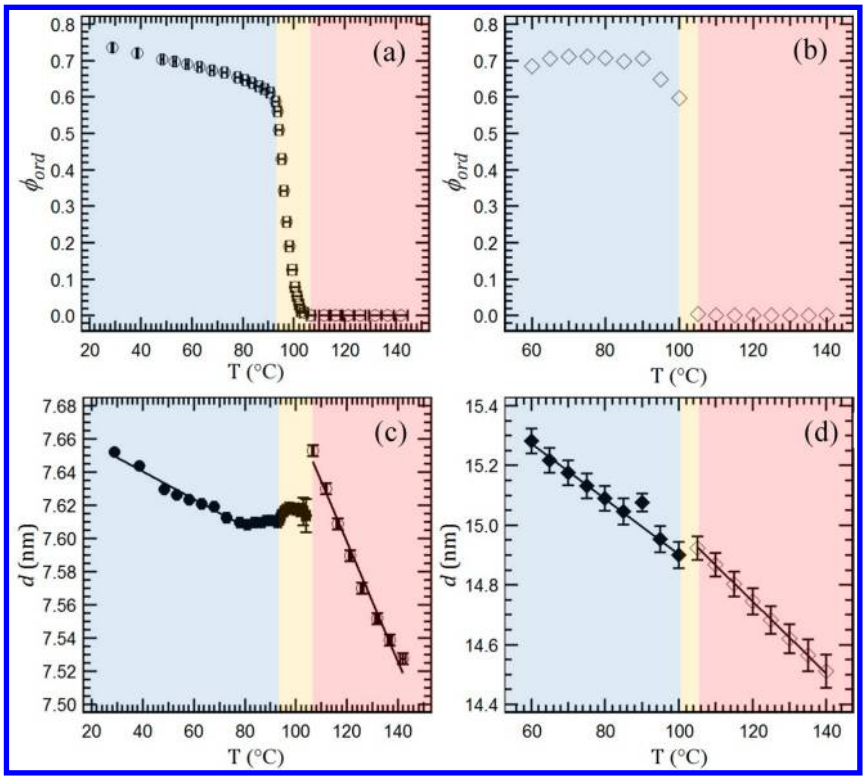

Figure 5. Temperature dependence of the calculated volume fraction of the ordered phase (ϕ_{ord}) for samples with (a) and without (b) LiTFSI salt added. The corresponding characteristic domain spacing as a function of temperature for the sample with (c) and without (d) salt added. In parts c and d, filled symbols correspond to the ordered lamellar domain spacing, open symbols indicate the characteristic spacing from the disordered melt, and the solid lines represent linear fits to the d vs T data. In all graphs, regions shaded in blue indicate temperatures below the ODT, regions in yellow encompass the occurrence of an ODT, and regions in red correspond to a fully disordered polymer melt. X-axis error bars indicate the range of temperatures measured between the front and back of the sample, and y-axis error bars correspond to one standard deviation in the fitting of the SAXS profiles.

of temperature between 83 and 91 °C. The coexistence window (93−104 °C) is relatively narrow and it is not easy to discern the temperature dependence of d_{ord} in this temperature range from Figure 5c; we will soon show that d_{ord} increases with increasing temperature in the coexistence window. An abrupt change is seen in Figure 5c at 107 °C. At temperatures greater than 107 °C, d_{dis} decreases rapidly with increasing temperature; the slope $d(d_{dis})/dT$ is -3.61×10^{-3} nm K^{-1}, a factor of about 5 greater than $d(d_{ord})/dT$ in the ordered window. The temperature dependence of d_{ord} and d_{dis} of the neat SEO(6.4−7.3) polymer shown in Figure 5d is unremarkable. The domain spacings decrease monotonically with increasing temperature (except for one outlier). The slopes $d(d_{ord})/dT$

dx.doi.org/10.1021/ma500292n | Macromolecules 2014, 47, 2666−2673

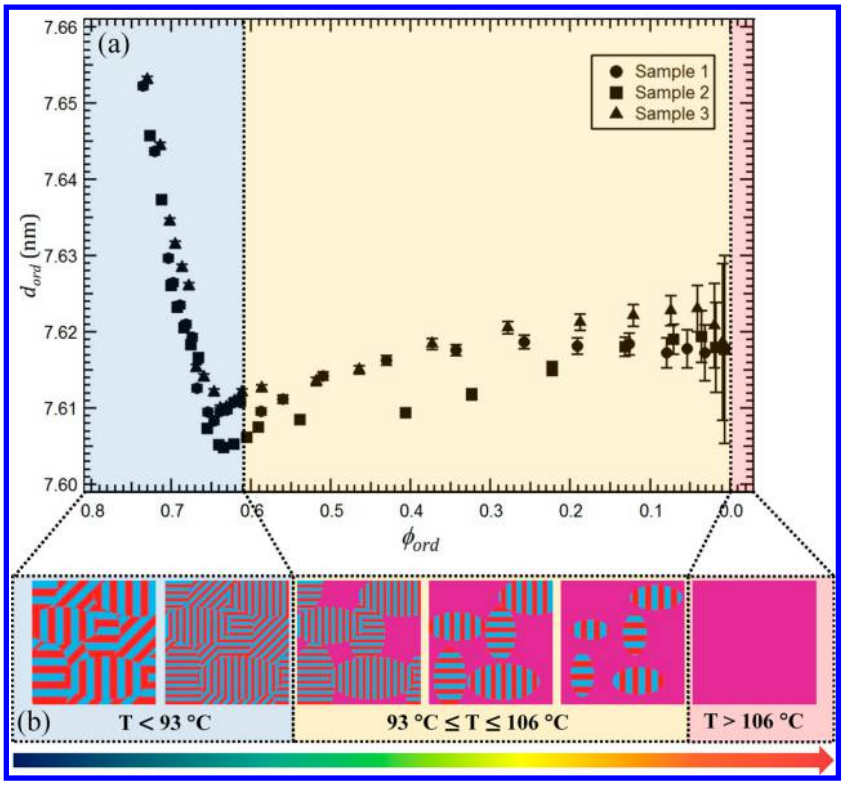

Figure 6. (a) $\phi_{ord}(T)$ and $d_{ord}(T)$ data plotted as d_{ord} vs ϕ_{ord}. y-axis error bars correspond to one standard deviation in the fitting of the SAXS profiles. (b) Exaggerated pictorial representation of the phase behavior observed for SEO(1.7−1.4)/LiTFSI(r = 0.075) throughout the experimental temperature range. Regions shaded in blue indicate temperatures below the ODT, regions in yellow encompass the coexistence region, and regions in red correspond to a fully disordered polymer melt.

and $d(d_{dis})/dT$ are -9.2×10^{-3} and -1.2×10^{-2} nm K^{-1}, respectively, values within 30% of each other.

The data obtained from the salt-containing block copolymer sample in Figures 5a and 5c in the ordered and coexistence windows are combined in Figure 6, where d_{ord} is plotted as a function of ϕ_{ord}. The absolute magnitude of the changes in domain spacings reported in Figure 5c is small. To ensure the robustness of our conclusions we studied three independent salt-containing block copolymer mixtures. Figure 6a shows the results obtained from all of our samples. The coexistence temperature windows obtained from the independent samples differed by ∼2−4 °C. Nevertheless, data obtained from these samples are quantitatively similar when plotted on a d_{ord} versus ϕ_{ord} plot. A particular advantage of this format is that it enables an expanded view of the coexistence window. The decrease of domain spacing with temperature in the ordered phase followed by an increase of domain spacing with temperature in the coexistence window is observed in all samples. We propose that the increase in domain spacing with temperature in the coexistence window is a signature of salt partitioning predicted by Nakamura et al.[20] Their theory leads to the interesting conclusion that the order parameter of the ordered phase in the coexistence temperature window would be larger than that in the fully ordered temperature window. This is because the salt concentration in the ordered domains in the coexistence window is greater than the concentration in the fully ordered window. Our experiments do not enable determination of the order parameter. However, one might infer local salt concentration from the measured domain spacing of the ordered lamellae. Young and Epps first reported a power-law increase in the domain spacing of an ordered SEO block copolymer with increasing salt concentration.[29] Figure 6b shows an exaggerated pictorial representation of changes in the sample morphology of SEO(1.7−1.4)/LiTFSI(r = 0.075) over the entire experimental temperature range. At low temperatures, the sample is fully ordered with large domain spacings that decrease with temperature. However, once the polymer begins to disorder within the coexistence window, the remaining lamellae become increasingly concentrated with salt. This partitioning of salt has two effects: it swells the lamellar domains by simple volume expansion, and the increased salt content in the lamellar phase increases the effective repulsion between the two blocks. It is important to note that stabilization of the ordered phase in the coexistence window is entirely due to salt partitioning, as noted by Nakamura et al.[20] At temperatures higher than the coexistence window, the salt concentration in the SEO(1.7−1.4)/LiTFSI(r = 0.075) sample becomes spatially uniform and the temperature dependence of the domain spacing is similar to that seen in neat diblock copolymers (Figure 5d).

The increase in d_{ord} with increasing temperature seen in the coexistence temperature window of the salt-containing block copolymer (Figure 6a) is a striking departure from the well-established behavior of neat block copolymers (Figure 5d). Most of the published literature on neat, nearly monodisperse block copolymers is consistent with the data presented in this paper.[8,10] A notable exception is the work of Koga et al. who reported a coexistence window of ∼2 °C in a neat block copolymer and observed temperature-dependent domain spacings similar to the data obtained from the salt-containing block copolymer sample reported in this study.[7] Coexistence

dx.doi.org/10.1021/ma500292n | Macromolecules 2014, 47, 2666−2673

windows with widths of ∼2 °C were also reported by Lee et al.[10]

CONCLUSIONS

We have studied the structural changes that occur in a block copolymer/salt mixture undergoing ODT using SAXS. In contrast to neat block copolymers, which show an abrupt change in SAXS scattering denoting the ODT, block copolymer/salt mixtures show a gradual transition from order to disorder over a finite temperature range. SAXS profiles within this temperature window appear to be the superposition of a sharp and a broad primary scattering peak, consistent with the coexistence of ordered and disordered phases. By fitting the scattering profiles and calculating the integrated scattering intensity contributions from each phase, we show that the ODT for block copolymer/salt mixtures is first order and occurs over a ∼11 °C window.

We gained further insight into the nature of the ODT in block copolymer/salt mixtures by analyzing the characteristic domain spacings (d_{ord}, d_{dis}) obtained from the SAXS profiles. Whereas the domain spacings in the neat block copolymer decrease monotonically with temperature, the block copolymer/salt mixture demonstrated an increase in d_{ord} with temperature within the ODT temperature window. We attribute this swelling of the ordered domain to the partitioning of salt within the lamellar microdomains in the coexistence window, as predicted by Nakamura et al.[20]

ASSOCIATED CONTENT

Supporting Information

Temperature dependent ionic conductivity and SAXS profile fitting parameters for the SEO(1.7−1.4)/LiTFSI(r = 0.075) samples. This material is available free of charge via the Internet at http://pubs.acs.org.

AUTHOR INFORMATION

Corresponding Author

*(N.P.B.) E-mail: nbalsara@berkeley.edu.

Present Address

#(I.N.) State Key Laboratory of Polymer Physics and Chemistry, Changchun Institute of Applied Chemistry, Chinese Academy of Sciences, Changchun, 130022, P. R. China

Notes

The authors declare no competing financial interest.

ACKNOWLEDGMENTS

This work was supported by the National Science Foundation, Grants DMR-0966626 and DMR-0966765. SAXS experiments were performed at Lawrence Berkeley National Laboratory's Advance Light Source, Beamline 7.3.3. Beamline 7.3.3 of the Advanced Light Source is supported by the Director of the Office of Science, Office of Basic Energy Sciences, of the U.S. Department of Energy under Contract No. DE-AC02-05CH11231.

NOMENCLATURE

Abbreviations

EIS	electrochemical impedance spectroscopy
LiTFSI	lithium bis(trifluoromethanesulfonyl)imide
ODT	order−disorder transition
PDI	polydispersity index
PEO	poly(ethylene oxide)
PS	polystyrene
SAXS	small angle X-ray scattering
SEO	polystyrene-*b*-poly(ethylene oxide) diblock copolymer
SPE	solid polymer electrolyte
THF	tetrahydrofuran

Symbols

A	index for component one of *A*−*B* block copolymer
b_A	scattering length of component A, cm
b_B	scattering length of component B, cm
B	index for component two of A−B block copolymer
C	effective scattering contrast of disordered polymer or polymer/salt mixture, nm^{-1}
d	characteristic domain spacing, nm
d_{dis}	characteristic domain spacing of disordered phase, nm
d_{ord}	characteristic domain spacing of ordered phase, nm
f_A	volume fraction of block A in an A−B block copolymer
$f_{EO,eff}$	effective volume fraction of poly(ethylene oxide) block and LiTFSI mixture
$g(f)$	form factor for a Gaussian chain
I	scattering intensity, cm^{-1}
$I_{bgd}(q)$	fit background scattering intensity, cm^{-1}
$I_{dis}(q)$	fit disordered phase scattering intensity, cm^{-1}
$I_{dis}\chi_{=0}(q)$	fit disordered phase scattering intensity with $\chi_{eff} = 0$ in eq 3, cm^{-1}
$I_{ord}(q)$	fit ordered phase scattering intensity, cm^{-1}
$I_{tot}(q)$	fit total scattering intensity, cm^{-1}
$\Delta I_{dis}(q)$	disordered phase scattering contribution, cm^{-1}
k	PDI correction factor constant
M_{PEO}	number-average molecular weight of PEO block, g mol^{-1}
M_{PS}	number-average molecular weight of PS block, g mol^{-1}
N	number-average degree of polymerization, sites $chain^{-1}$
q	scattering vector, nm^{-1}
q^*	primary ordered scattering peak location, nm^{-1}
Q	total integrated scattering intensity, $cm^{-1}nm^{-3}$
Q_i	phase-specific integrated scattering intensity, $cm^{-1}nm^{-3}$
ΔQ	disordered phase integrated scattering intensity, $cm^{-1}nm^{-3}$
r	salt concentration, $[Li^+][EO]^{-1}$
R_g	radius of gyration, nm
$S(q)$	sum element of the structure factor matrix
$S_{AA}(q)$	A−A pairwise element of the structure factor matrix,
$S_{AB}(q)$	A−B pairwise element of the structure factor matrix
$S_{BB}(q)$	B−B pairwise element of the structure factor matrix
T_g^{PS}	glass transition temperature of the poly(styrene) block, °C
ν_A	monomer volume for component A, cm^3
ν_B	monomer volume for component B, cm^3
ν_{ref}	reference volume, cm^3
w	Gaussian peak width, nm^{-1}
$W(q)$	determinant element of the structure factor matrix
x	nondimensional length
y_0	constant in eq 2, cm^{-1}
y_1	constant in eq 15, cm^{-1}
y_2	constant in eq 15, nm^{-1}

Greek

χ	Flory−Huggins interaction parameter

χ_{eff} Effective interaction parameter for copolymer/salt mixture
ϕ_{ord} Ordered phase volume fraction
λ Scattering wavelength, nm
θ Scattering angle, rad

REFERENCES

(1) Agrawal, R. C.; Pandey, G. P. Solid Polymer Electrolytes: Materials Designing and All-Solid-State Battery Applications: An Overview. *J. Phys. D: Appl. Phys.* **2008**, *41*, 223001.
(2) Hallinan, D. T.; Mullin, S. A.; Stone, G. M.; Balsara, N. P. Lithium Metal Stability in Batteries with Block Copolymer Electrolytes. *J. Electrochem. Soc.* **2013**, *160*, A464−A470.
(3) Tarascon, J. M.; Armand, M. Issues and Challenges Facing Rechargeable Lithium Batteries. *Nature* **2001**, *414*, 359−367.
(4) Panday, A.; Mullin, S. A.; Gomez, E. D.; Wanakule, N. S.; Chen, V. L.; Hexemer, A.; Pople, J.; Balsara, N. P. Effect of Molecular Weight and Salt Concentration on Conductivity of Block Copolymer Electrolytes. *Macromolecules* **2009**, *42*, 4632−4637.
(5) Leibler, L. Theory of Microphase Separation in Block Copolymers. *Macromolecules* **1980**, *13*, 1602−1617.
(6) Mai, S.; Fairclough, J. P. A.; Hamley, I. W.; Matsen, M. W.; Denny, R. C.; Liao, B.; Booth, C.; Ryan, A. J. Order−Disorder Transition in Poly(oxyethylene)−Poly(oxybutylene) Diblock Copolymers. *Macromolecules* **1996**, *29*, 6212−6221.
(7) Koga, T.; Koga, T.; Hashimoto, T. Ultra-Small-Angle X-Ray Scattering Studies on Order-Disorder Transition in Diblock Copolymers. *J. Chem. Phys.* **1999**, *110*, 11076−11086.
(8) Sakamoto, N.; Hashimoto, T. Order-Disorder Transition of Low Molecular Weight Polystyrene-Block-Polyisoprene. 1. SAXS Analysis of Two Characteristic Temperatures. *Macromolecules* **1995**, *28*, 6825−6834.
(9) Mori, K.; Okawara, A.; Takeji, H. Order-Disorder Transition of Polystyrene-Block-Polyisoprene. I. Thermal Concentration Fluctuations in Single-Phase Melts and Solutions and Determination of X as a Function of Molecular Weight and Composition. *J. Chem. Phys.* **1996**, *104*, 7765.
(10) Lee, S.; Gillard, T. M.; Bates, F. S. Fluctuations, Order, and Disorder in Short Diblock Copolymers. *AIChE* **2013**, *59*, 3502−3513.
(11) Floudas, G.; Pakula, T.; Fischer, E. W.; Hadjichristidis, N.; Pispas, S. Ordering Kinetics in a Symmetric Diblock Copolymer. *Acta Polym.* **1994**, *45*, 176−181.
(12) Hammond, M. R.; Cochran, E.; Fredrickson, G. H.; Kramer, E. J. Temperature Dependence of Order, Disorder, and Defects in Laterally Confined Diblock Copolymer Cylinder Monolayers. *Macromolecules* **2005**, *38*, 6575−6585.
(13) Fredrickson, G. H.; Helfand, E. Fluctuation Effects in the Theory of Microphase Separation in Block Copolymers. *J. Chem. Phys.* **1987**, *87*, 697.
(14) Wanakule, N. S.; Virgili, J. M.; Teran, A. A.; Wang, Z.-G.; Balsara, N. P. Thermodynamic Properties of Block Copolymer Electrolytes Containing Imidazolium and Lithium Salts. *Macromolecules* **2010**, *43*, 8282−8289.
(15) Nakamura, I.; Balsara, N. P.; Wang, Z.-G. Thermodynamics of Ion-Containing Polymer Blends and Block Copolymers. *Phys. Rev. Lett.* **2011**, *107*, 198301.
(16) Nakamura, I.; Wang, Z.-G. Salt-Doped Block Copolymers: Ion Distribution, Domain Spacing and Effective X Parameter. *Soft Matter* **2012**, *8*, 9356−9367.
(17) Gunkel, I.; Thurn-Albrecht, T. Thermodynamic and Structural Changes in Ion-Containing Symmetric Diblock Copolymers: A Small-Angle X-Ray Scattering Study. *Macromolecules* **2012**, *45*, 283−291.
(18) Majewski, P. W.; Gopinadhan, M.; Jang, W.; Lutkenhaus, J. L.; Osuji, C. O. Anisotropic Ionic Conductivity in Block Copolymer Membranes by Magnetic Field Alignment. *J. Am. Chem. Soc.* **2010**, *132*, 17516−17522.
(19) Teran, A. A.; Balsara, N. P. Thermodynamics of Block Copolymers with and without Salt. *J. Phys. Chem. B* **2014**, *118*, 4−17.
(20) Nakamura, I.; Balsara, N. P.; Wang, Z. First-Order Disordered-to-Lamellar Phase Transition in Lithium Salt-Doped Block Copolymers. *ACS Macro Lett.* **2013**, *2*, 478−481.
(21) Quirk, R. P.; Kim, J.; Kausch, C.; Chun, M. Butyllithium-Initiated Anionic Synthesis of Well-Defined Poly(styrene-Block-Ethylene Oxide) Block Copolymers with Potassium Salt Additives. *Polym. Int.* **1996**, *39*, 3−10.
(22) Hadjichristidis, N.; Iatrou, H.; Pispas, S.; Pitsikalis, M. Anionic Polymerization: High Vacuum Techniques. *J. Polym. Sci. Part A Polym. Chem.* **2000**, *38*, 3211−3234.
(23) Yuan, R.; Teran, A. A.; Gurevitch, I.; Mullin, S. A.; Wanakule, N. S.; Balsara, N. P. Ionic Conductivity of Low Molecular Weight Block Copolymer Electrolytes. *Macromolecules* **2013**, *46*, 914−921.
(24) Hexemer, A.; Bras, W.; Glossinger, J.; Schaible, E.; Gann, E.; Kirian, R.; MacDowell, A.; Church, M.; Rude, B.; Padmore, H. A SAXS/WAXS/GISAXS Beamline with Multilayer Monochromator. *J. Phys. Conf. Ser.* **2010**, *247*, 012007.
(25) Teran, A. A.; Mullin, S. A.; Hallinan, D. T.; Balsara, N. P. Discontinuous Changes in Ionic Conductivity of a Block Copolymer Electrolyte through an Order−Disorder Transition. *ACS Macro Lett.* **2012**, *1*, 305−309.
(26) Ilavsky, J. Nika: Software for Two-Dimensional Data Reduction. *J. Appl. Crystallogr.* **2012**, *45*, 324−328.
(27) Roe, R.-J. *Methods of X-Ray and Nuetron Scattering in Polymer Science*; Oxford University Press Inc.: 2000.
(28) De Gennes, P. G. Theory of X-Ray Scattering by Liquid Macromolecules with Heavy Atom Labels. *J. Phys. (Paris)* **1970**, *31*, 235−238.
(29) Young, W.; Epps, T. H. Salt Doping in PEO-Containing Block Copolymers: Counterion and Concentration Effects. *Macromolecules* **2009**, *42*, 2672−2678.